Mathematical model of pennate muscle (LIF043-15)

Wiktoria Wojnicz, Bartłomiej Zagrodny, Michał Ludwicki,
Jan Awrejcewicz, Edmund Wittbrodt

Abstract: The purpose of this study is to create a new mathematical model of pennate striated skeletal muscle. This new model describes behaviour of isolated flat pennate muscle in two dimensions (2D) by taking into account that rheological properties of muscle fibres depend on their planar arrangement. A new mathematical model is implemented in two types: 1) numerical model of unipennate muscle (unipennate model); 2) numerical model of bipennate muscle (bipennate model). Applying similar boundary conditions and similar load, proposed numerical models had been tested. Obtained results were compared with results of numerical researches by applying a Hill-Zajac muscle model (this is a Hill type muscle model, in which the angle of pennation is taken into consideration) and a fusiform muscle model (a muscle is treated as a structure composed of serially linked different mechanical properties parts).

1. Introduction

The human movement system consists of striated skeletal muscles that have different architectures. Among these muscles are fusiform muscles and pennate muscles (unipennate muscles, bipennate muscles and multipennate muscles) [7]. The fusiform muscle fibers run generally parallel to the muscle axis (it is line connecting the origin tendon and the insertion tendon). The unipennate muscle fibers run parallel to each other but at the pennation angle to the muscle axis [6]. The bipennate muscle consists of two unipennate muscles that run in two distinct directions (i.e. different pennation angles). The multipennate muscle is composed of a few bundles of fibers that run in distinct directions.

From the physiology point of view the unipennate muscle consists of three parts: the muscle insertion (‘muscle – insertion tendon’ connection), the belly (muscle fibers), and the muscle origin (‘muscle – origin tendon’ connection). It is assumed that during contraction the belly maintains the isovolume, each tendon moves only along its axis and muscle fibers become more pennated (the pennation angle is increased) [12].

The spatial arrangement of pennate muscle fibres determines the muscle fibres length, the lengths of tendons and mechanical properties of muscle. That is why the contractile characteristic (i.e. force-generating capacity) depends on the pennation angle [6]. Moreover, one should take into consideration that a real pennate muscle is a non-homogenous structure: the distal muscle fascicles

tend to contract more (i.e. they act at greater pennation angles) than the more proximal muscle fascicles.

Applying an imaging techniques, such as nuclear magnetic resonance (MRI) and ultrasonography (US), with a motion analysis techniques, one might perform *in vivo* non-invasive measurements to estimate volumes of muscles, muscle fibres lengths and pennation angles [6]. However, one should perform invasive measurements to obtain [1]: 1) mechanical properties values (by applying tensile tests and sonomicrometry); 2) muscle morphology and architecture evaluated at the microscopic level (by using a muscle biopsy); 3) muscle static characteristic (length-force dependence); 4) muscle dynamic characteristic (velocity-force dependence); 5) muscle-tendon parameters used in the Hill-type muscle model. That is why a very limited amount of data describing mechanical properties of pennation muscles can be found in literature.

To model behaviour of pennate muscle one should take into consideration that spatial arrangement of muscle fibers influence mechanical properties and contractile properties of this muscle. Nowadays, to describe pennate muscle function in muscle biomechanics there are applied rheological models: Hill-type muscle models and Hill-Zajac muscle models [4,12]. However, application of these models is very limited due to problems related to the obtainment of model parameters.

The purpose of this study is to create a new mathematical model of pennate striated skeletal muscle that describes behaviour of isolated flat pennate muscle in two dimensions (2D) by taking into account that rheological properties of muscle fibres depend on their planar arrangement. A new mathematical model is implemented in two types: 1) numerical model of unipennate muscle (unipennate model); 2) numerical model of bipennate muscle (bipennate model).

2. Pennate muscle modelling

2.1 Principles of modelling

The mathematical models of unipennate muscle and bipennate muscle were created on the base of a deformation schema of unipennate muscle shown in the Figure 1. According to this deformation schema, the muscle contraction occurs in the plane (two-dimension space) along muscle fibers directed at the pennation angle α_p towards the line connecting the muscle insertion (it is a movable part with one degree of freedom) and the muscle origin (it is a non-movable part). It is assumed that during muscle contraction the muscle width *tt* is constant (according to [5]) and muscle fibers generate a contractile muscle force F_m, which causes the displacement of muscle insertion *x* and counterbalances an external force F_{ext}:

$$F_{ext} = F_m \cdot cos\alpha_p \,. \tag{1}$$

During contraction the muscle fibers are shortening and the muscle insertion is translated from the point B to the point B' (the distance BB' is equal to x). It causes the change of pennation angle: the initial value of pennation angle α_{po} (at the length of muscle equals AB), is changed to the value α_p (at the length of muscle equals AB'). Analyzing the deformation schema of unipennate muscle, the following relation can be derived:

$$tt = AB \cdot cos\alpha_{po} = AB' \cdot cos\alpha_p \ . \tag{2}$$

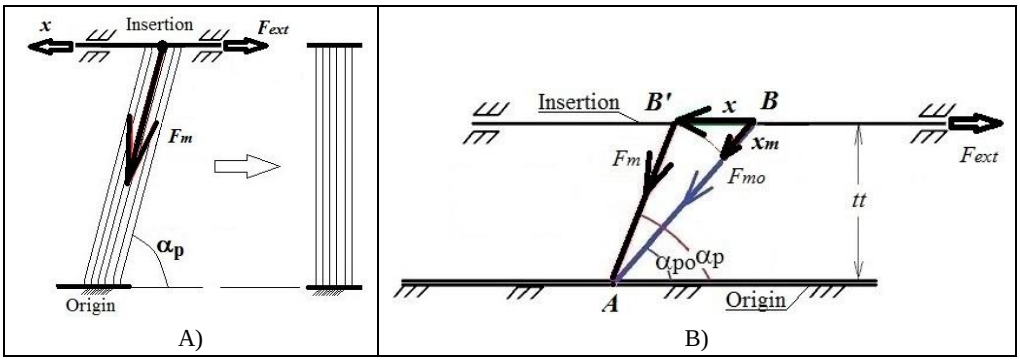

Figure 1. Deformation schema of unipennate muscle:
A) directions of acting of external force F_{ext} and contractile muscle force F_m towards the muscle insertion displacement x; B) schema of deformation of unipennate muscle (AB – the initial length of muscle (before contraction); AB' – the finish length of muscle (after contraction); F_{mo} – initial contractile muscle force at the length of muscle equals AB; F_m – finish contractile muscle force at the length of muscle equals AB'; α_{po} – the pennation angle before contraction (at the length of muscle equals AB); α_p – the pennation angle after contraction (at the length of muscle equals AB'); x_m – change of muscle length that is equal to the difference of the length AB and the length AB').

Taking into consideration a deformation schema of unipennate muscle, five rheological models were created:

1) Unipennate muscle model WW (the author is Wiktoria Wojnicz) (part 2.2);
2) Unipennate muscle model BZ (the author is Batłomiej Zagrodny) (part 2.3);
3) Hill-Zajac unipennate muscle model (part 2.4);
4) The bipennate muscle model WW (the author is Wiktoria Wojnicz) (part 2.5);
5) The bipennate muscle model BZ (the author is Batłomiej Zagrodny) (part 2.6).

Assuming that the time variable is t, proposed models can be applied to solve the dynamics task formulated in three following problems:

1) Input variables are the insertion displacement $x(t)$ and the external force $F_{ext}(t)$; output variables are the internal force $P^W(t)$ (this force is generated by the contractile elements of muscle model and it causes an appearing of contractile muscle force $F_m(t)$), the pennation angle $\alpha_p(t)$ and deformations of muscle model parts (for chosen muscle models);

2) Input variables are the insertion displacement $x(t)$ and the internal force $P^w(t)$; output variables are the external force $F_{ext}(t)$, the pennation angle $\alpha_p(t)$ and deformations of muscle model parts (for chosen muscle models);
3) Input variables are the external force $F_{ext}(t)$ and the internal force $P^w(t)$; output variables are the insertion displacement $x(t)$, the pennation angle $\alpha_p(t)$ and deformations of muscle model parts (for chosen muscle models).

2.2. Unipennate muscle model WW

The unipennate muscle model WW describes behaviour of unipennate muscle with the pennation angle equals α_p (Figure 2). This muscle behaviour is described by the rheological model created on the base of the rheological model of fusiform muscle published in [10,11]. The rheological model of unipennate muscle model WW is composed of serially linked three fragments (two passive (non-contractile) fragments and one active (contractile) fragment) that describe different mechanical properties of muscle parts. Each fragment is composed of mass element, elastic element and viscous element. Active fragment has additionally a contractile element that models an ability of muscle to contract. Two lateral fragments model the passive muscle parts (muscle-tendon connections of the muscle insertion and the muscle origin). One middle fragment models the active muscle part (i.e. muscle belly). This model has three degrees of freedom. According to this model: 1) the difference of displacements ($x_0 - x_1$) describes the change of upper passive muscle fragment; 2) the difference of displacements ($x_1 - x_2$) describes the change of middle active muscle fragment; 3) the displacement x_2 describes the change of lower passive muscle fragment.

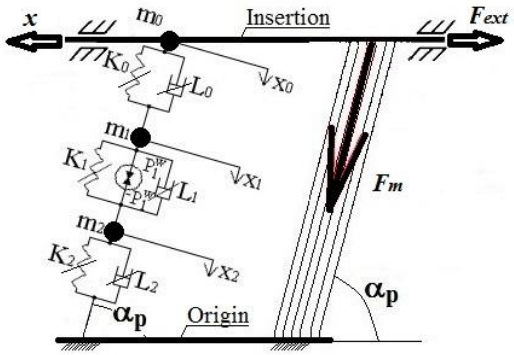

Figure 2. Unipennate muscle model WW (rheological model).

The mathematical model of the unipennate muscle model WW is described by the system of three differential equations:

$$
\begin{aligned}
&m_0 \cdot \ddot{x} + L_0 \cdot (\dot{x}_0 - \dot{x}_1) \cdot cos\alpha_p + K_0 \cdot (x_0 - x_1) \cdot cos\alpha_p = -F_{ext}(t) \\
&m_1 \cdot \ddot{x}_1 + L_0 \cdot (\dot{x}_1 - \dot{x}_0) + K_0 \cdot (x_1 - x_0) + L_1 \cdot (\dot{x}_1 - \dot{x}_2) + K_1 \cdot (x_1 - x_2) = P_1^w(t) \\
&m_2 \cdot \ddot{x}_2 + L_1 \cdot (\dot{x}_2 - \dot{x}_1) + K_1 \cdot (x_2 - x_1) + L_2 \cdot \dot{x}_2 + K_2 \cdot x_2 = -P_1^w(t)
\end{aligned}, \tag{3}
$$

and following geometrical relations:

$$
\alpha_p = arcsin\left(\frac{l_0 \cdot sin\alpha_{po}}{l_0 - x_0}\right), \tag{4A}
$$

$$
x_0 = l_0 + \frac{x \cdot cos\alpha_{po} - l_0}{cos(\alpha_p - \alpha_{po})}, \tag{4B}
$$

$$
\dot{x}_0 = \frac{dx_0}{dt} = \frac{\dot{x} \cdot cos\alpha_{po}}{cos(\alpha_p - \alpha_{po}) - A(x_0) \cdot sin(\alpha_p - \alpha_{po}) \cdot (x_0 - l_0)}, \tag{4C}
$$

$$
A(x_0) = \frac{l_0 \cdot sin\alpha_{po}}{(l_0 - x_0)^2} \cdot \frac{1}{\sqrt{1 - \left(\frac{l_0 \cdot sin\alpha_{po}}{l_0 - x_0}\right)^2}}, \tag{4D}
$$

where: m_j – mass of the j-th element; K_j – stiffness coefficient of the j-th elastic element; L_j – damping coefficient of the j-th viscous element; $P_1^w(t)$ – internal force of the contractile element; l_0 – initial length of muscle model; α_{po} – initial pennation angle when the length of muscle model is equals to l_0.

2.3. Unipennate muscle model BZ

The unipennate muscle model BZ describes behaviour of unipennate muscle with the pennation angle equals α_p (Figure 3). This model is similar to the unipennate muscle model WW (part 2.2). The unipennate muscle model BZ takes into consideration that stiffness and dumping characteristics of skeletal muscle is described by a nonlinear relationship according to [2,9]:

1) $K_j = k_j \cdot x_j^2$, j = w, z, 1,2, where k_j is a correction factor of stiffness;

2) $C_j = c_j \cdot \dot{x}_j^2$, j = w, z, 1, 2, where c_j is a correction factor of damping.

Applying the geometrical relations (4A – 4D), the mathematical model of unipennate muscle model BZ is described by the system of two following equations:

$$
\begin{aligned}
&m_w \cdot \ddot{x}_w + C_w \cdot \dot{x}_w + K_w \cdot x_w - \frac{C_z \cdot (\dot{x}_z - \dot{x}_1) + K_z \cdot (x_z - x_1)}{cos\alpha_p} = P_w(t) \\
&m_z \cdot \ddot{x}_z - C_z \cdot (\dot{x}_z - \dot{x}_1) - K_z \cdot (x_z - x_z) = -F_{ext}(t)
\end{aligned}, \tag{5}
$$

where: $x_1 = x_w \cdot cos\alpha_p$; x_w – displacement of mass m_w; x_z – displacement of mass m_z.

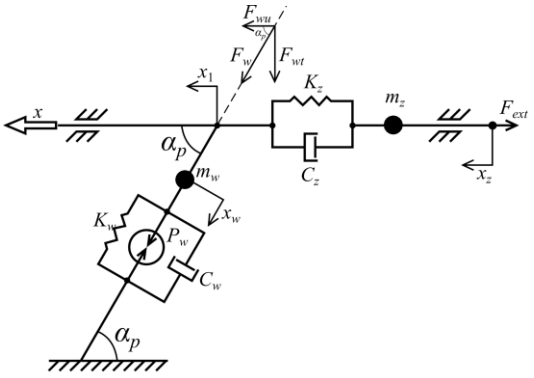

Figure 3. Unipennate muscle model BZ.

2.4. Hill-Zajac unipennate muscle model

The Hill-Zajac unipennate muscle model describes behaviour of unnipennate muscle by using the Hill-type muscle model and Zajac muscle model (this is a Hill type muscle model, in which the angle of pennation α_p is taken into consideration). There are a lot of modifications of these models [4,12]. In this paper it was assumed that Hill-Zajac unipennate muscle model has a rheological structure shown in the Figure 4. In this model the muscle length is the sum of belly length $L_m/\cos(\alpha_p)$ and tendon length L_t. Mechanical properties of muscle are described by using a mass element M (this is a muscle mass reduced to a point) and parallel linking of three elements: a contractile element that generates a force F_{CE} (it depends on the actual muscle length l, velocity of muscle fibers contraction and activation Act that originate from a nervous system), a parallel elastic element described by a stiffness coefficient equals K_{PE} and a viscous element described by a damping coefficient equals L. Tendon behaviour is modelled by using an elastic element and its force depends on the tendon stiffness coefficient K_t and the tendon elongation described by a difference of displacements $(x_t - x)$.

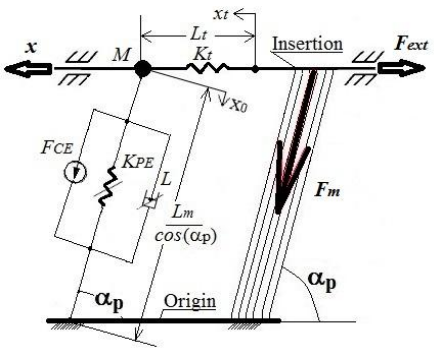

Figure 4. Hill-Zajac unipennate muscle model (rheological model).

The mathematical model of Hill-Zajaca unipennate muscle model is described by the system of two equations:

$$\begin{array}{l} F_{ext} + K_t \cdot (x - x_t) = 0 \\ M \cdot \ddot{x} + K_t \cdot (x - x_t) = F_m \cdot cos\alpha_p \end{array}, \quad (6)$$

where the contractile muscle force is equals to:

$$F_m = F_{CE} - K_{PE} \cdot x_0 - L \cdot \dot{x}_0 . \quad (7)$$

It was assumed that force of contractile element F_{CE} depends on the muscle activation *Act*, the muscle length *l* and difference between the active component of static muscle characteristic F_m^{act} and the passive component of static muscle characteristic F_m^{pas}:

$$F_{CE} = Act \cdot \left(F_m^{act}(l) - F_m^{pas}(l) \right). \quad (8)$$

To implement the Hill-Zajac unipennate muscle model there were used: 1) a static muscle characteristic (length-force relationship) proposed in [5]; 2) a static tendon characteristic (elongation-force relationship) proposed in [12]; 3) a dynamic muscle characteristic (velocity-force relationship) published in [12]; 4) data described musculotendon properties (the maximum isometric muscle force, the optimal muscle fiber length, the tendon slack length) according with [5].

2.5. Bipennate muscle model WW

The bipennate muscle model WW described behaviour of bipennate muscle composed of two parts directed at the pennation angle α_{p1} (left part with a constant muscle width tt_1) and the pennation angle α_{p2} (right part with a constant muscle width tt_2) towards the muscle insertion (it is movable part) and muscle origins (there are non-movable parts) (Figure 5). Each muscle part behaviour is modelled as a rheological model of the unipennate muscle WW described in the part 2.2 (i.e. each muscle part is composed of two passive fragments and one active fragment). The bipennate muscle model WW has six degrees of freedom. According to this model: 1) difference of displacements ($x_{01} - x_{11}$) describes the length change of upper passive fragment of muscle left part; 2) difference of displacements ($x_{11} - x_{21}$) describes the length change of middle active fragment of muscle left part; 3) displacement x_{21} describes the length change of lower passive fragment of muscle left part; 4) difference of displacements ($x_{02} - x_{12}$) describes the length change of upper passive fragment of muscle right part; 5) difference of displacements ($x_{12} - x_{22}$) describes the length change of middle active fragment of muscle right part; 6) displacement x_{22} describes the length change of lower passive fragment of muscle right part.

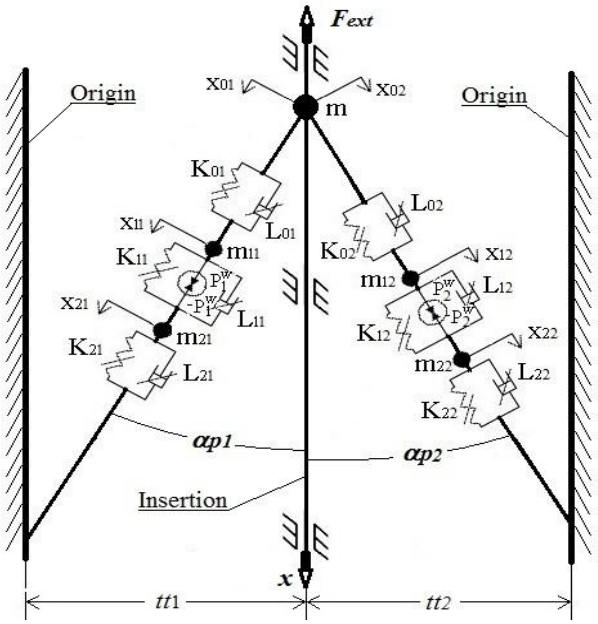

Figure 5. Bipennate muscle model WW (rheological model).

The mathematical model of bipennate muscle model WW is described by the system of five differential equations:

$$\begin{aligned}
&m\cdot\ddot{x}+L_{01}\cdot(\dot{x}_{01}-\dot{x}_{11})\cdot cos\alpha_{p1}+K_{01}\cdot(x_{01}-x_{11})\cdot cos\alpha_{p1}+\\
&\quad+L_{02}\cdot(\dot{x}_{02}-\dot{x}_{12})\cdot cos\alpha_{p2}+K_{02}\cdot(x_{02}-x_{12})\cdot cos\alpha_{p2}=-F_{ext}(t)\\
&m_{11}\cdot\ddot{x}_{11}+L_{01}\cdot(\dot{x}_{11}-\dot{x}_{01})+K_{01}\cdot(x_{11}-x_{01})+L_{11}\cdot(\dot{x}_{11}-\dot{x}_{21})+K_{11}\cdot(x_{11}-x_{21})=P_1^w(t)\\
&m_{21}\cdot\ddot{x}_{21}+L_{11}\cdot(\dot{x}_{21}-\dot{x}_{11})+K_{11}\cdot(x_{21}-x_{11})+L_{21}\cdot\dot{x}_{21}+K_{21}\cdot x_{21}=-P_1^w(t)\\
&m_{12}\cdot\ddot{x}_{12}+L_{02}\cdot(\dot{x}_{12}-\dot{x}_{02})+K_{02}\cdot(x_{12}-x_{02})+L_{12}\cdot(\dot{x}_{12}-\dot{x}_{22})+K_{12}\cdot(x_{12}-x_{22})=P_2^w(t)\\
&m_{22}\cdot\ddot{x}_{22}+L_{12}\cdot(\dot{x}_{22}-\dot{x}_{12})+K_{12}\cdot(x_{22}-x_{12})+L_{22}\cdot\dot{x}_{22}+K_{22}\cdot x_{22}=-P_2^w(t)
\end{aligned}, \tag{9}$$

and following geometrical relations:

$$\alpha_{p1}=arcsin\left(\frac{l_{01}\cdot sin\alpha_{p1}}{l_{01}-x_{01}}\right),\quad \alpha_{p2}=arcsin\left(\frac{l_{02}\cdot sin\alpha_{p2}}{l_{02}-x_{02}}\right), \tag{10A}$$

$$x_{01}=l_{01}+\frac{x\cdot cos\alpha_{p1}-l_{01}}{cos(\alpha_{p1}-\alpha_{po1})},\quad x_{02}=l_{02}+\frac{x\cdot cos\alpha_{p2}-l_{02}}{cos(\alpha_{p2}-\alpha_{po2})}, \tag{10B}$$

$$\begin{aligned}
\dot{x}_{01}&=\frac{dx_{01}}{dt}=\frac{\dot{x}\cdot cos\alpha_{p1}}{cos(\alpha_{p1}-\alpha_{po1})-A(x_{01})\cdot sin(\alpha_{p1}-\alpha_{po1})\cdot(x_{01}-l_{01})}\\
\dot{x}_{02}&=\frac{dx_{02}}{dt}=\frac{\dot{x}\cdot cos\alpha_{p2}}{cos(\alpha_{p2}-\alpha_{po2})-A(x_{02})\cdot sin(\alpha_{p2}-\alpha_{po2})\cdot(x_{02}-l_{02})}
\end{aligned}, \tag{10C}$$

$$A(x_{01}) = \frac{l_{01} \cdot sin\alpha_{p1}}{(l_{01} - x_{01})^2} \cdot \frac{1}{\sqrt{1 - \left(\frac{l_{01} \cdot sin\alpha_{p1}}{l_{01} - x_{01}}\right)^2}}$$
$$A(x_{02}) = \frac{l_{02} \cdot sin\alpha_{p2}}{(l_{02} - x_{02})^2} \cdot \frac{1}{\sqrt{1 - \left(\frac{l_{02} \cdot sin\alpha_{p2}}{l_{02} - x_{02}}\right)^2}}, \quad (10D)$$

where: m_{ji} – mass of the *j*-th element of *i*-th muscle part; m – mass of the element m_{01} and the element m_{02}; K_{ji} – stiffness coefficient of the *j*-th elastic element of *i*-th muscle part; L_{ji} – damping coefficient of the *j*-th viscous element of *i*-th muscle part; $P_1^w(t)$ – internal force of the contractile element of left muscle part; $P_2^w(t)$ – internal force of the contractile element of right muscle part; l_{01} – initial length of left part of muscle model; l_{02} – initial length of right part of muscle model; α_{po1} – initial pennation angle when the length of left part of muscle model is equal to l_{01}; α_{po2} – initial pennation angle when the length of right part of muscle model is equal to l_{02}.

2.6. Bipennate muscle model BZ

The bipennate muscle model BZ described behaviour of bipennate muscle directed at the pennation angle α (left part) and the pennation angle β (right part) towards the muscle insertion (it is movable part) and muscle origins (there are non-movable parts) (Figure 6).

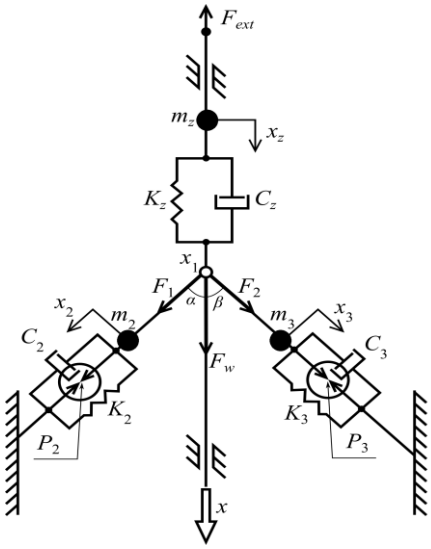

Figure 6. Bipennate muscle model BZ.

The bipennate muscle model BZ is similar to the bipennate muscle model WW (part 2.5) but it takes into consideration that stiffness and dumping characteristics of skeletal muscle are nonlinear (part. 2.3). Applying the geometrical relationships (10A – 10D), the mathematical model of bipennate muscle model BZ is described by the system of four following equations:

$$\begin{aligned} &m_z \cdot \ddot{x}_z + C_z \cdot (\dot{x}_z - \dot{x}_1) + K_z \cdot (x_z - x_1) = -F_{ext}(t) \\ &m_2 \cdot \ddot{x}_2 + C_2 \cdot \dot{x}_2 + K_2 \cdot x_2 = P_2(t) + F_1(t) \\ &m_3 \cdot \ddot{x}_3 + C_3 \cdot \dot{x}_3 + K_3 \cdot x_3 = P_3(t) + F_2(t) \\ &F_1(t) \cdot cos\alpha + F_2(t) \cdot cos\beta = C_z \cdot (\dot{x}_z - \dot{x}_1) + K_z \cdot (x_z - x_1), \end{aligned} \tag{11}$$

where: $x_1 = x2 \cdot cos\alpha = x_3 \cdot cos\beta$.

3. Numerical simulation results

Numerical models of unipennate muscle and bipennate muscle were created on the base of proposed mathematical models. To perform numerical researches there were used data describing a lateral head of triceps brachii published in [5]. Applying similar boundary conditions and similar load, proposed numerical models had been tested. Numerical model of unipennate muscle model WW (described in part 2.2) was applied to solve three problems of the dynamics task described in part 2.1. Chosen results obtained from numerical solving of the third problem are shown at the Figure 7.

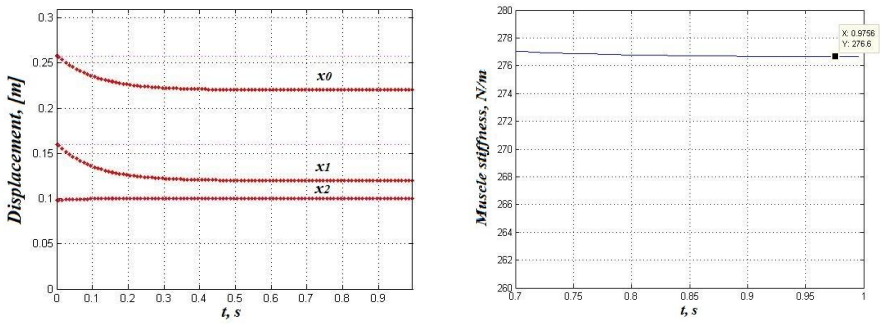

A) B)

Figure 7. Numerical simulation results of the unipennate muscle model WW: A) displacement of muscle points; B) stiffness of muscle.

Numerical model of Hill-Zajac unipennate muscle model (described in part 2.4) was applied to solve a dynamics task formulated in the following problem: input variables are the insertion displacement $x(t)$, the pennation angle $\alpha_p(t)$ and the external force $F_{ext}(t)$; output variables are the force of contractile element F_{CE} and muscle activation *Act.* Chosen results obtained from numerical solving of this problem are shown at the Figure 8.

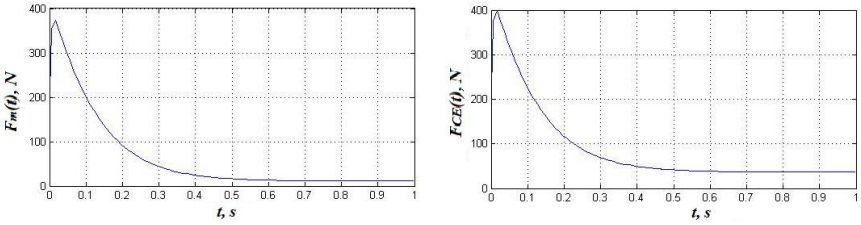

Figure 8. Numerical simulation results of the Hill-Zajac unipennate muscle model: contractile muscle force F_m and force of contractile element F_{CE}.

Numerical model of bipennate muscle model WW (described in part 2.5) was applied to solve the third problem of the dynamics task (described in part 2.1). Chosen results obtained from numerical solving of the third problem are shown in the Figure 9.

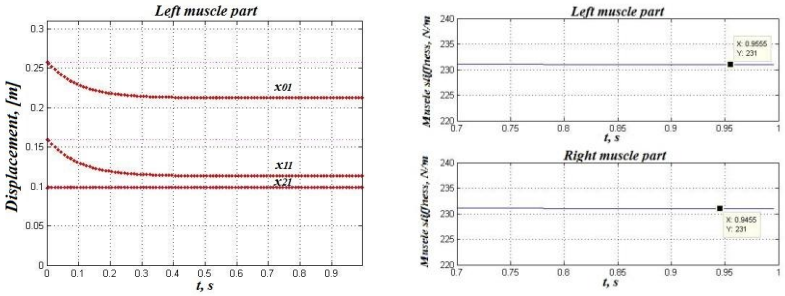

A) B)

Figure 9. Numerical simulation results of the bipennate muscle model WW: A) displacement of left muscle part points; B) stiffness of muscle left and right part.

Numerical model of unipennate muscle model BZ (described in part 2.3) and bipennate muscle model BZ (described in part 2.6) were applied to solve the third problem of the dynamics task (described in part 2.1). Chosen results obtained from numerical solving of the third problem are shown in the Figure 10.

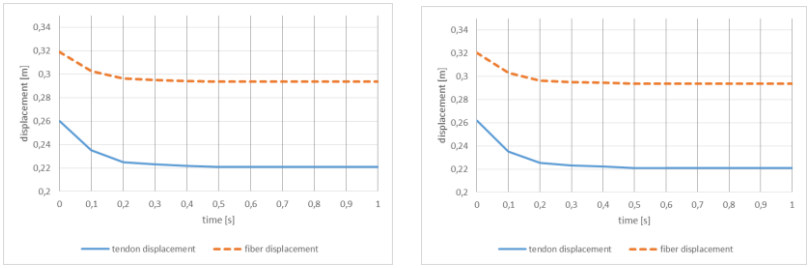

A) B)

Figure 10. Numerical simulation results of: A) the unipennate muscle model BZ (displacement of the tendon x_z and muscle fiber x_w; B) the bipennate muscle model BZ (displacement of the tendon x_z and muscle fibers $x_2 = x_3$ in the case of $\alpha = \beta$).

To compare the influence of planar arrangement of muscle fibers the numerical model of fusiform muscle model published in [11] was applied to solve the third problem of the dynamics task (chosen results are shown in the Figure 11).

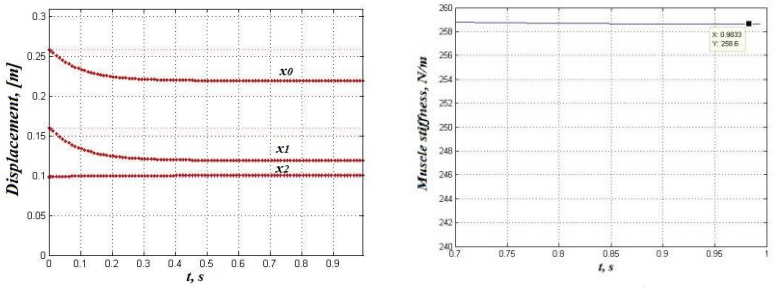

A) B)

Figure 11. Numerical simulation results of the fusiform muscle model: A) displacement of muscle points; B) stiffness of muscle.

4. Method of verification

To prove models proposed in this paper a method of verification was elaborated. According to this method, a first step consists in applying a non-invasive image analysis and a second step consists in performing experiments by using the prototype of pennate muscle. An image analysis (US or MRI) allows us to perform static image analysis (for a single image) and dynamical image analysis (for a multiple images or a single movie). It is worth noticing that an image analysis requires that an image has high resolution to precisely distinguish muscle fibers [3,8]. Single image of muscle section allows to measure a pennation angle α_p, a muscle diameter and a muscle length (Figure 12).

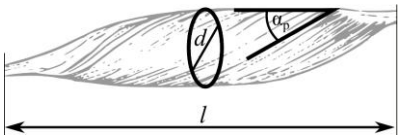

Figure 12. Muscle geometrical parameters in visual analysis: pennation angle α_p, muscle diameter d and muscle length l.

The prototype of pennate muscle is composed of four artificial pneumatic muscles (Figure 13). Each artificial muscle is a linear McKibben actuator. This prototype allows us to form four initial pennation angles: 9^o, 14^o, 18^o and 24^o. Chosen experiments results and numerical simulation results are shown in the Figure 14. Analysing these results, we may conclude that greater pennation angle causes the drop of force measured along a long axis of the muscle (each pneumatic actuator produces the same maximal force, which is independent of the pennation angle).

Figure 13. A prototype of pennate muscle (a prototype is composed of four artificial pneumatic muscles)

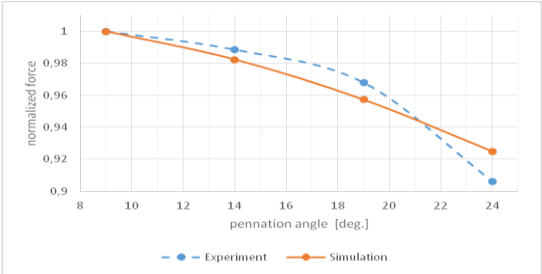

Figure 14. Normalized force as a function of pennation angle.

5. Conclusions

The aim of this study was to create mathematical models of unipennate striated skeletal muscle and bipennate striated skeletal muscle. New models were created in the form of rheological models by taking into consideration that muscle contraction occurs in two-dimension space and the arrangement of muscle fibers influence mechanical properties and contractile properties of this muscle. Moreover, at this stage of modelling we assumed that slow and fast muscle tissues have identical mechanical properties.

Analysing results of numerical simulations we concluded that:

1) efficiency of fusiform muscle (it is a quotient the external force to the contractile muscle force) is more than the efficiency of unipennate muscle (because a unipennate muscle works in a plane and a part of its contractile force is devoted to spatial arrangement of muscle fibers);
2) the efficiency of bipennate muscle is more that the efficiency of unipennate muscle;
3) to model a behaviour of pennate muscle one should precisely describe the geometrical relations occurring between pennate muscle fibers (i.e. geometrical constrains) and the force-length relations depended on the time variable (i.e. dynamics equations of motion).

Acknowledgments

The numerical simulations had been performed using computers of "Centrum Informatyczne Trójmiejskiej Akademickiej Sieci Komputerowej" in Gdansk, Poland.

References

[1] Aagaard P., Andersen J.L., Poulsen P.D., Leffers A.M., Wagner A., Magnussin S.P., Kristensen J.H., Simonsen E.B. A mechanism for increased contractile strength of human pennate muscle

in response to strength training: changes in muscle architecture. *Journal of Physiology* 534.2, 2001, pp.613-623

[2] Awrejcewicz J., Kudra G., Zagrodny B. Nonlinearity of muscle stiffness. *Theoretical and Applied Mechanics Letters* 2(5), 2012, pp. 1-3

[3] Csapo R., Malis V., Hodgson J., Sinha S. Age-related greater Achilles tendon compliance is not associated with larger plantar flexor muscle fascicle strains in senior women. *Journal of Applied Physiology* 116 (8), 2014, pp. 961–969

[4] Delp S.L. *Surgery simulation – a computer graphics system to analyze and design musculoskeletal reconstructions of the lower limb*. PhD. thesis, Stanford University Press, 1990, Stanford, Zajac F.

[5] Garner B.A., Pandy M.G. Estimation of musculotendon properties in the human upper limb. *Annals of Biomedical Engineering* 31, 2003, pp. 207-220

[6] Narici M. Human skeletal muscle architecture studied in vivo by non-invasive imaging techniques: functional significance and applications. *Journal of Electromyography and Kinesiology* 9, 1999, pp. 97-103

[7] Nigg B.M., Herzog W. Biomechanics of the musculoskeletal system. John Wiley & Sons, 1994, Chichester

[8] Noorkoiv M., Stavnsbo A., Aagaard P., Blazevich A.J. In vivo assessment of muscle fascicle length by extended field-of-view ultrasonography, *Journal of Applied Physiology* 109 (6), 2010, pp. 1974–1979.

[9] Soderberg G.L. Kinesiology: Application to pathological motion, Baltimore, Williams & Wilkins, 1986.

[10] Wojnicz W., Wittbrodt E. Analysis of muscles' behaviour. Part I. The computational model of muscle. *Acta of Bioengineering and Biomechanics* 11, 2009, pp. 15-21

[11] Wojnicz W., Wittbrodt E. Application of muscle model to the musculoskeletal modeling. *Acta of Bioengineering and Biomechanics* 14, 2012, pp. 29-39

[12] Zajac F. Muscle and tendon: properties, models, scaling and application to biomechanics and motor control. *Critical Reviews in Biomedical Engineering* 17, 1989, pp. 359-410

Wiktoria Wojnicz, Ph.D.: Gdansk University of Technology, str. G. Narutowicza 11/12, 80-233 Gdansk, POLAND (wiktoria.wojnicz@pg.gda.pl). The author gave a presentation of this paper during one of the conference sessions.

Bartłomiej Zagrodny, Ph.D.: Lodz University of Technology, str. Stefanowskiego 1/15 , 90-924 Lodz, POLAND (bartlomiej.zagrodny@p.lodz.pl).

Michał Ludwicki, Ph.D.: Lodz University of Technology, str. Stefanowskiego 1/15 , 90-924 Lodz POLAND (michal.ludwicki@p.lodz.pl).

Jan Awrejcewicz, Professor: Lodz University of Technology, str. Stefanowskiego 1/15 , 90-924 Lodz, POLAND (jan.awrejcewicz@p.lodz.pl).

Edmund Wittbrodt, Professor: Gdansk University of Technology, str. G. Narutowicza 11/12, 80-233 Gdansk, POLAND (e.wittbrodt@pg.gda.pl).